PERGAMON

International Journal of Solids and Structures 40 (2003) 4789–4812

INTERNATIONAL JOURNAL OF SOLIDS and STRUCTURES

www.elsevier.com/locate/ijsolstr

Exact dynamic solutions to piezoelectric smart beams including peel stresses I: Theory and application

Liyong Tong *, Quantian Luo

School of Aerospace, Mechanical and Mechatronic Engineering, The University of Sydney, Bldg J11, Sydney, NSW 2006, Australia

Received 1 September 2002; received in revised form 28 April 2003

Abstract

This work presents exact dynamic solutions to piezoelectric (PZT) smart beams including peel stresses. The governing equations of partial differential forms are firstly derived for a PZT smart beam made of the identical adherends, and then general solutions of the governing equations are studied. The analytical solutions are applied to a cantilever beam with a partially bonded PZT patch to the fixed end. For the given boundary conditions, exact solutions of the steady state motions are obtained. Based on the exact solutions, frequency spectra, natural frequencies, normal mode shapes, harmonic responses of the shear and peel stresses are discussed for the PZT actuator. The details of the numerical results and sensing electric charges will be presented in Part II of this work. The exact dynamic solutions can be directly applied to a PZT bimorph bender. To compare with the classic shear lag model whose numerical demonstrations will be given in Part II, the related equations are also derived for the shear lag rod model and shear lag beam model.

Keywords: Smart beam; Dynamic analysis; Shear and peel stresses; Piezoelectric bimorph

1. Introduction

Dynamic control for flexible smart structures has drawn a significant attention in the past decades. In our previous work on exact static solutions (Luo and Tong, 2002a,b), it was shown that piezoelectric (PZT) beam models taking into account both shear and peel stresses in adhesive are more accurate than the classical shear lag model, especially for flexible structures. To better understand dynamic behaviors of smart structures, we will develop exact solutions for dynamics of piezoelectric smart beams considering peel stresses in this work.

To obtain the exact dynamic solutions, we consider a smart beam in Fig. 1, whose composite part is made of the identical substrates or adherends. This special type of piezoelectric devices is called the PZT

* Corresponding author. Tel.: +61-2-93516949; fax: +61-2-93514841.
E-mail address: ltong@aeromech.usyd.edu.au (L. Tong).

0020-7683/03/$ - see front matter © 2003 Elsevier Ltd. All rights reserved.
doi:10.1016/S0020-7683(03)00264-6

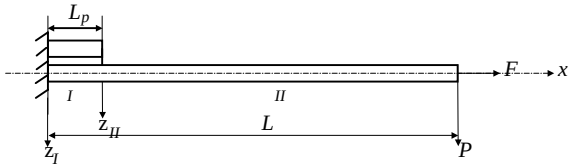

Fig. 1. A smart beam with a bonded PZT patch.

bimorphs, which have been widely used as displacement transducers or actuators in precise sub-micron increments and in active vibration or noise control.

Smits et al. (1991) presented an extensive review for the PZT bimorph applications, in which, they derived the constitutive equations for the PZT bimorph bender using the internal energy density of infinitesimal volume elements in thermodynamic equilibrium in the presence of a voltage on the electrodes. Kugel et al. (1998) developed a new type of bimorph-based piezoelectric air transducer with a frequency range of 200–1000 Hz. Morris and Forster (2000) discussed the optimization of a circular piezoelectric bimorph for a micro-pump driver. Lim et al. (2001) studied three-dimensional responses for parallel piezoelectric bimorphs. In these investigations, adhesive layer was not taken into account in the formulations of all models and peel stress along through the thickness direction was not considered.

This paper is not intended to study design and applications of PZT bimorphs, and instead focuses on developing analytical solutions of dynamics applicable to PZT bimorphs. In the demonstrated examples, it can be deemed as the simplest bimorph that is formed by bonding a PZT patch to the top surface of a host beam and the obtained dynamic solutions can be tailored to study the dynamic and static analysis of a PZT bimorph bender.

Crawley and de Luis (1987) developed a theoretical framework for a smart beam with bonded or embedded PZT patches. In their dynamic analysis, they considered the case for which the PZT patches were assumed to be very thin compared with the host beam, and thus the static results of shear stresses and the actuated equivalent forces can be directly used as the excitation functions by ignoring the PZTs' mass.

Gibbs and Fuller (1992) presented an approximate analytical model for the excitation of a thin beam, in which no adhesive layer was considered and the actuated equivalent forces were discussed. Irschik et al. (1999) presented a new class of shaped piezoelectric sensors for deflection measurements. Rizet et al. (2000) developed an active control system for controlling the flexural vibration of a smart beam, whose results indicated that the simple analytical model was not very accurate and the first two resonant frequencies predicted by the finite element method were lower than those of the experiment.

A dynamic smart beam model will be presented on the basis of our static model by including the PZT mass. Using the concept of equivalent forces, we will also develop an approximate solution procedure for the dynamic analysis of PZT smart beams by considering peel stress distributions in Part II, in which, the application and limitations of the dynamic equivalent forces will be investigated by comparing the exact dynamic solutions with the approximate ones.

2. Motion equations and solutions of a smart beam

Consider a smart beam with a bonded PZT patch as shown in Fig. 1. It is assumed that the patch and host beam have identical material and geometrical properties.

2.1. Non-dimensional motion equations

To derive non-dimensional forms of dynamic equations for the PZT patch and the host beam, we introduce the following non-dimensional parameters:

$$\left.\begin{aligned}
&u_{n1}=\frac{u_1}{h},\quad w_{n1}=\frac{w_1}{h},\quad u_{nh}=\frac{u_h}{h},\quad w_{nh}=\frac{w_h}{h},\quad \xi=\frac{x}{L_p},\quad t_n=\frac{t}{T},\quad \Omega=\frac{\omega}{\omega_T},\quad \omega_T=\frac{1}{T}=\frac{1}{L_p}\sqrt{\frac{E_h}{\rho}}\\
&E_{nh}=\frac{E_h}{G_a},\quad \tau_n=\frac{\tau}{G_a},\quad \sigma_n=\frac{\sigma}{G_a},\quad r_h=\frac{h}{L_p},\quad m_n=m_T\omega_T^2,\quad m_T=\frac{mh}{G_a},\quad r_{\tau a}=\frac{h}{t_a},\quad r_{\sigma a}=\frac{E_a}{G_a}\frac{h}{t_a}\\
&N_{n1}=\frac{N_1}{G_a h},\quad N_{nh}=\frac{N_h}{G_a h},\quad M_{n1}=\frac{M_1}{G_a L_p h},\quad M_{nh}=\frac{M_h}{G_a L_p h},\quad Q_{n1}=\frac{Q_1}{G_a h},\quad Q_{nh}=\frac{Q_h}{G_a h}
\end{aligned}\right\} \tag{1}$$

Some of the above parameters are different from those defined in our static analysis (Luo and Tong, 2002a,b) for convenient formulations. In Eq. (1), E_h is the elastic modulus of the adherends; m and ρ are the density, mass per unit length and per unit volume respectively; L_p is the length of the PZT patch; E_a and G_a are the elastic and shear moduli of the adhesive layer. Definitions of remaining symbols are given in Figs. 1 and 2. The subscript n in all equations refers to non-dimensional quantities.

Referring to Fig. 2 and Eq. (1), we have dynamic equations:

$$r_h\frac{\partial N_{n1}}{\partial\xi}+\tau_n=m_n\frac{\partial^2 u_{n1}}{\partial t_n^2},\quad r_h\frac{\partial Q_{n1}}{\partial\xi}+\sigma_n=m_n\frac{\partial^2 w_{n1}}{\partial t_n^2},\quad \frac{\partial M_{n1}}{\partial\xi}+\frac{1}{2}\tau_n-Q_{n1}=0 \tag{2}$$

$$r_h\frac{\partial N_{nh}}{\partial\xi}-\tau_n=m_n\frac{\partial^2 u_{nh}}{\partial t_n^2},\quad r_h\frac{\partial Q_{nh}}{\partial\xi}-\sigma_n=m_n\frac{\partial^2 w_{nh}}{\partial t_n^2},\quad \frac{\partial M_{nh}}{\partial\xi}+\frac{1}{2}\tau_n-Q_{nh}=0 \tag{3}$$

On the basis of the *Euler–Bernoulli* beam theory (Timoshenko and Gere, 1972), the piezoelectricity theory (Tiersten, 1969) and the model of adhesive joints developed by Goland and Reissner (1944), the constitutive relations of the PZT patch, the host beam, which may also be a PZT material, and the adhesive layer are:

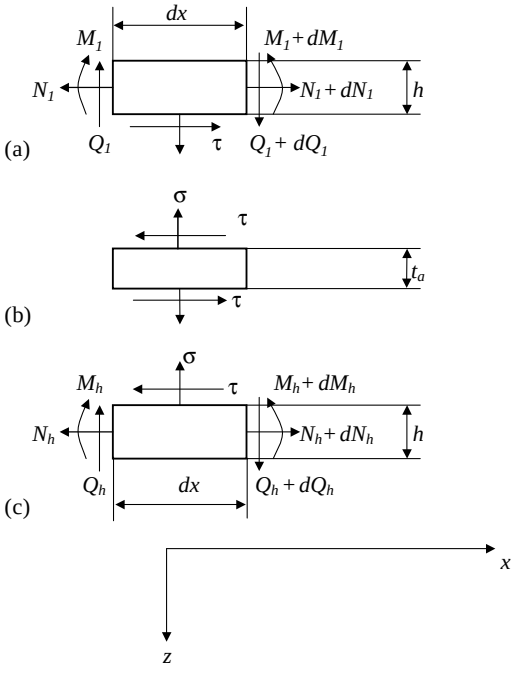

Fig. 2. Free body diagrams of the infinitesimal elements. (a) PZT infinitesimal element, (b) the adhesive element and (c) host beam infinitesimal element.

$$\left.\begin{aligned}
&N_{n1} = E_{nh} r_h \frac{\partial u_{n1}}{\partial \xi} + \frac{e_{31} V_1(t)}{G_a h} \\
&M_{n1} = -\frac{1}{12} E_{nh} r_h^3 \frac{\partial^2 w_{n1}}{\partial \xi^2} \\
&\tau_n = r_{\tau a}\left[(u_{nh} - u_{n1}) + \frac{r_h}{2}\left(\frac{\partial w_{nh}}{\partial \xi} + \frac{\partial w_{n1}}{\partial \xi}\right)\right], \quad \sigma_n = r_{\sigma a}(w_{nh} - w_{n1}) \\
&N_{nh} = E_{nh} r_h \frac{\partial u_{nh}}{\partial \xi} + \frac{e_{31} V_h(t)}{G_a h} \\
&M_{nh} = -\frac{1}{12} E_{nh} r_h^3 \frac{\partial^2 w_{nh}}{\partial \xi^2}
\end{aligned}\right\} \tag{4}$$

where e_{31} is a coupling piezoelectric constant; V_h and V_1 are voltages. In Eqs. (2)–(4), effects of the rotational inertia and shear strains are neglected in light of the *Euler–Bernoulli* beam theory and the unit width of the beam cross section with a rectangular shape is assumed.

Substituting Eq. (4) into Eqs. (2) and (3), we can obtain the motion equations:

$$\left.\begin{aligned}
&E_{nh} r_h^2 \frac{\partial^2 u_{n1}}{\partial \xi^2} + r_{\tau a}\left[(u_{nh} - u_{n1}) + \frac{r_h}{2}\left(\frac{\partial w_{nh}}{\partial \xi} + \frac{\partial w_{n1}}{\partial \xi}\right)\right] = m_n \frac{\partial^2 u_{n1}}{\partial t_n^2} \\
&E_{nh} r_h^2 \frac{\partial^2 u_{nh}}{\partial \xi^2} - r_{\tau a}\left[(u_{nh} - u_{n1}) + \frac{r_h}{2}\left(\frac{\partial w_{nh}}{\partial \xi} + \frac{\partial w_{n1}}{\partial \xi}\right)\right] = m_n \frac{\partial^2 u_{nh}}{\partial t_n^2} \\
&-\frac{E_{nh} r_h^4}{12}\frac{\partial^4 w_{n1}}{\partial \xi^4} + \frac{r_{\tau a} r_h}{2}\left[\left(\frac{\partial u_{nh}}{\partial \xi} - \frac{\partial u_{n1}}{\partial \xi}\right) + \frac{r_h}{2}\left(\frac{\partial^2 w_{nh}}{\partial \xi^2} + \frac{\partial^2 w_{n1}}{\partial \xi^2}\right)\right] + r_{\sigma a}(w_{nh} - w_{n1}) = m_n \frac{\partial^2 w_{n1}}{\partial t_n^2} \\
&-\frac{E_{nh} r_h^4}{12}\frac{\partial^4 w_{nh}}{\partial \xi^4} + \frac{r_{\tau a} r_h}{2}\left[\left(\frac{\partial u_{nh}}{\partial \xi} - \frac{\partial u_{n1}}{\partial \xi}\right) + \frac{r_h}{2}\left(\frac{\partial^2 w_{nh}}{\partial \xi^2} + \frac{\partial^2 w_{n1}}{\partial \xi^2}\right)\right] - r_{\sigma a}(w_{nh} - w_{n1}) = m_n \frac{\partial^2 w_{nh}}{\partial t_n^2}
\end{aligned}\right\} \tag{5}$$

2.2. General solutions to partial differential forms of the motion equations

To solve partial differential equations shown in Eq. (5), we first simplify it using the following transformations:

$$\left.\begin{aligned}
&2u_s = u_{nh} + u_{n1}, \quad 2N_s = N_{nh} + N_{n1}, \quad 2w_s = w_{nh} - w_{n1}, \quad 2Q_s = Q_{nh} - Q_{n1}, \quad 2M_s = M_{nh} - M_{n1} \\
&2u_a = u_{nh} - u_{n1}, \quad 2N_a = N_{nh} - N_{n1}, \quad 2w_a = w_{nh} + w_{n1}, \quad 2Q_a = Q_{nh} + Q_{n1}, \quad 2M_a = M_{nh} + M_{n1} \\
&2V_s = V_h + V_1, \quad 2V_a = V_h - V_1
\end{aligned}\right\} \tag{6}$$

By utilizing the above transformations, Eqs. (4) and (5) become:

$$N_s = E_{nh} r_h \frac{\partial u_s}{\partial \xi} + \frac{e_{31} V_s(t)}{G_a h}, \quad M_s = -\frac{E_{nh} r_h^3}{12}\frac{\partial^2 w_s}{\partial \xi^2}, \quad \sigma_n = 2 r_{\sigma a} w_s \tag{7}$$

$$\left.\begin{aligned}
&E_{nh} r_h^2 \frac{\partial^2 u_s}{\partial \xi^2} = m_n \frac{\partial^2 u_s}{\partial t_n^2} \\
&-\frac{E_{nh} r_h^4}{12}\frac{\partial^4 w_s}{\partial \xi^4} - 2 r_{\sigma a} w_s = m_n \frac{\partial^2 w_s}{\partial t_n^2}
\end{aligned}\right\} \tag{8}$$

$$N_a = E_{nh} r_h \frac{\partial u_a}{\partial \xi} + \frac{e_{31} V_a(t)}{G_a h}, \quad M_a = -\frac{E_{nh} r_h^3}{12}\frac{\partial^2 w_a}{\partial \xi^2}, \quad \tau_n = 2 r_{\tau a}\left(u_a + \frac{r_h}{2}\frac{\partial w_a}{\partial \xi}\right) \tag{9}$$

$$\left.\begin{aligned} &E_{nh}r_h^2\frac{\partial^2 u_a}{\partial\xi^2}-2r_{\tau a}\left(u_a+\frac{r_h}{2}\frac{\partial w_a}{\partial\xi}\right)=m_n\frac{\partial^2 u_a}{\partial t_n^2}\\ &-\frac{E_{nh}r_h^4}{12}\frac{\partial^4 w_a}{\partial\xi^4}+2r_{\tau a}\frac{r_h}{2}\left(\frac{\partial u_a}{\partial\xi}+\frac{r_h}{2}\frac{\partial^2 w_a}{\partial\xi^2}\right)=m_n\frac{\partial^2 w_a}{\partial t_n^2}\end{aligned}\right\} \tag{10}$$

The uncoupled differential equation (8) can be easily solved and the coupled equation (10) can also be solved analytically. Once Eqs. (8) and (10) are solved, the dynamic shear and peel stresses are obtained using Eqs. (7) and (9), and the dynamic solutions to extensional and flexural motions of the PZT and the host beam can be obtained through the transformations defined in Eq. (6).

When the harmonic motions are assumed, solutions to Eq. (8) become:

$$u_s=U_s(\xi)\sin\Omega t_n,\quad w_s=W_s(\xi)\sin\Omega t_n \tag{11}$$

and the vibration amplitudes $U_s(\xi)$ and $W_s(\xi)$ can be found:

$$U_s=A_{s1}\sin\beta_{s1}\xi+A_{s2}\cos\beta_{s1}\xi \tag{12}$$

$$W_s=(B_{s1}\sinh\beta_e\xi+B_{s2}\cosh\beta_e\xi)\sin\beta_e\xi+(B_{s3}\sinh\beta_e\xi+B_{s4}\cosh\beta_e\xi)\cos\beta_e\xi,\quad \text{when } \omega<\alpha_s \tag{13}$$

$$W_s=(B_{s1}\xi^3+B_{s2}\xi^2+B_{s3}\xi+B_{s4}),\quad \text{when } \omega=\alpha_s \tag{14}$$

$$W_s=(B_{s1}\sinh\beta_{s2}\xi+B_{s2}\cosh\beta_{s2}\xi+B_{s3}\sin\beta_{s2}\xi+B_{s4}\cos\beta_{s2}\xi),\quad \text{when } \omega>\alpha_s \tag{15}$$

where

$$\beta_{s1}=\frac{\omega}{\alpha_u},\quad \beta_{s2}=\frac{\sqrt[4]{|\omega^2-\alpha_s^2|}}{\sqrt{\alpha_w}},\quad \beta_e=\frac{\sqrt{2}}{2}\beta_{s2},\quad \alpha_u=\sqrt{\frac{E_{nh}r_h^2}{m_T}},\quad \alpha_w=\sqrt{\frac{E_{nh}r_h^4}{12m_T}},\quad \alpha_s=\sqrt{\frac{2r_{\sigma a}}{m_T}} \tag{16}$$

To solve Eq. (10), we assume that:

$$u_a=U_a(\xi)\sin\Omega t_n=A_a e^{\beta\xi}\sin\Omega t_n,\quad w_a=W_a(\xi)\sin\Omega t_n=B_a e^{\beta\xi}\sin\Omega t_n \tag{17}$$

Substituting Eq. (17) into Eq. (10) yields the following characteristic equations:

$$\left.\begin{aligned} &[\alpha_u^2\beta^2+(\omega^2-\alpha_a^2)]A_a-\frac{r_h}{2}\beta\alpha_a^2B_a=0\\ &\frac{r_h}{2}\beta\alpha_a^2A_a-\left[\alpha_w^2\beta^4-\left(\frac{r_h^2}{4}\alpha_a^2\beta^2+\omega^2\right)\right]B_a=0\end{aligned}\right\} \tag{18}$$

The condition ensuring non-trivial solutions to u_a and w_a requires:

$$\lambda^3-[\beta_{aw}^2+(\beta_{au}^2-\beta_{\omega u}^2)]\lambda^2-(\beta_{\omega w}^2+\beta_{aw}^2\beta_{\omega u}^2)\lambda+\beta_{\omega w}^2(\beta_{au}^2-\beta_{\omega u}^2)=0 \tag{19}$$

In Eqs. (18) and (19),

$$\lambda=\beta^2,\quad \alpha_a=\sqrt{\frac{2r_{\tau a}}{m_T}},\quad \beta_{aw}=\frac{r_h\alpha_a}{2\alpha_w},\quad \beta_{au}=\frac{\alpha_a}{\alpha_u},\quad \beta_{\omega u}=\frac{\omega}{\alpha_u},\quad \beta_{\omega w}=\frac{\omega}{\alpha_w} \tag{20}$$

It can be shown that, the three roots of λ in Eq. (19) are all real numbers in normal cases of structural geometry, mass density and material properties. The solution forms of amplitudes U_a and W_a are:

$$\left.\begin{aligned} &U_a=A_{a1}\sinh\beta_1\xi+A_{a2}\cosh\beta_1\xi+A_{a3}\sinh\beta_2\xi+A_{a4}\cosh\beta_2\xi+A_{a5}\sin\beta_3\xi+A_{a6}\cos\beta_3\xi\\ &W_a=B_{a1}\sinh\beta_1\xi+B_{a2}\cosh\beta_1\xi+B_{a3}\sinh\beta_2\xi+B_{a4}\cosh\beta_2\xi+B_{a5}\sin\beta_3\xi+B_{a6}\cos\beta_3\xi\\ &\text{when } \omega<\alpha_a\end{aligned}\right\} \tag{21}$$

$$\left.\begin{aligned} U_a &= A_{a1}\sinh\beta_1\xi + A_{a2}\cosh\beta_1\xi + A_{a3}\sin\beta_2\xi + A_{a4}\cos\beta_2\xi + A_{a5}\xi + A_{a6} \\ W_a &= B_{a1}\sinh\beta_1\xi + B_{a2}\cosh\beta_1\xi + B_{a3}\sin\beta_2\xi + B_{a4}\cos\beta_2\xi + B_{a5}\xi + B_{a6} \\ &\text{when } \omega = \alpha_a \end{aligned}\right\} \tag{22}$$

$$\left.\begin{aligned} U_a &= A_{a1}\sinh\beta_1\xi + A_{a2}\cosh\beta_1\xi + A_{a3}\sin\beta_2\xi + A_{a4}\cos\beta_2\xi + A_{a5}\sin\beta_3\xi + A_{a6}\cos\beta_3\xi \\ W_a &= B_{a1}\sinh\beta_1\xi + B_{a2}\cosh\beta_1\xi + B_{a3}\sin\beta_2\xi + B_{a4}\cos\beta_2\xi + B_{a5}\sin\beta_3\xi + B_{a6}\cos\beta_3\xi \\ &\text{when } \omega > \alpha_a \end{aligned}\right\} \tag{23}$$

where $\beta_i = \sqrt{|\lambda_i|}$, $(i = 1, 2, 3)$; λ_i are the roots of Eq. (19); A_{ai} and B_{ai} $(i = 1, 2, \ldots, 6)$ are integration constants to be determined.

It can be seen that, the solution forms depend on the frequencies of the applied voltages or loadings, the material properties and the geometries of the adhesive and adherends. For example, assume the material properties and geometric parameters of the adherends and the adhesive to be: $m = \rho A_h = \rho h = 7800 \times 0.001$ kg/m; $E_a = 3.00$ Gpa; $G_a = 1.07$ Gpa and $t_a = 0.1$ mm, we have:

$$\alpha_a = \sqrt{\frac{2r_{\tau a}}{m_T}} = 1656379 \ (1/\mathrm{s})$$

If $\omega > \alpha_a$, it is related to the vibrations with very high frequencies. In practice, the lower frequencies are normally concerned. Therefore, we only consider dynamic solutions in the case that $\omega < \alpha_a$; in this case, ω is also less than α_s. The solutions are thus given by Eqs. (12), (13) and (21). The integration constants in these equations can be determined by the boundary conditions. To validate numerically the solution and study the PZT bimorph bender, we consider a host beam with the partially bonded PZT patch as shown in Fig. 1.

3. Exact solutions of a cantilever beam with the bonded PZT patch to the fixed end

3.1. Boundary conditions

The different expressions of motion equations for each section of the smart beam in Fig. 1 require the boundary conditions for each part. The boundary conditions of Section II are:

$$\left.\begin{aligned} \xi = 0 : \frac{\mathrm{d}U_{nh\mathrm{II}}}{\mathrm{d}\xi} &= \varepsilon_N \qquad \xi = \alpha_p = \frac{L - L_p}{L_p} : \frac{\mathrm{d}U_{nh\mathrm{II}}}{\mathrm{d}\xi} = \varepsilon_F \\ \frac{\mathrm{d}^2W_{nh\mathrm{II}}}{\mathrm{d}\xi^2} &= -\varepsilon_M \qquad\qquad\quad \frac{\mathrm{d}^2W_{nh\mathrm{II}}}{\mathrm{d}\xi^2} = 0 \\ \frac{\mathrm{d}^3W_{nh\mathrm{II}}}{\mathrm{d}\xi^3} &= -\varepsilon_Q \qquad\qquad\quad \frac{\mathrm{d}^3W_{nh\mathrm{II}}}{\mathrm{d}\xi^3} = -\varepsilon_P \end{aligned}\right\} \tag{24}$$

The boundary conditions of Section I are:

$$\left.\begin{aligned} \xi = 0 : U_{n1} = 0, \quad U_{nh} = 0 \qquad \xi = 1 : \frac{\mathrm{d}U_{n1}}{\mathrm{d}\xi} &= \varepsilon_p, \quad \frac{\mathrm{d}U_{nh}}{\mathrm{d}\xi} = \varepsilon_N \\ W_{n1} = 0, \quad W_{nh} = 0 \qquad\qquad \frac{\mathrm{d}^2W_{n1}}{\mathrm{d}\xi^2} &= 0, \quad \frac{\mathrm{d}^2W_{nh}}{\mathrm{d}\xi^2} = -\varepsilon_M \\ \frac{\mathrm{d}W_{n1}}{\mathrm{d}\xi} = 0, \quad \frac{\mathrm{d}W_{nh}}{\mathrm{d}\xi} = 0 \qquad\qquad \frac{\mathrm{d}^3W_{n1}}{\mathrm{d}\xi^3} &= \frac{6\tau_n}{E_{nh}r_h^3}, \quad \frac{\mathrm{d}^3W_{nh}}{\mathrm{d}\xi^3} = \frac{6\tau_n}{E_{nh}r_h^3} - \varepsilon_Q \end{aligned}\right\} \tag{25}$$

According to the relations defined in Eqs. (5) and (6), we have:

$$\left.\begin{array}{ll} \xi = 0 : U_s = 0 & \xi = 1 : \dfrac{\mathrm{d}U_s}{\mathrm{d}\xi} = \dfrac{1}{2}(\varepsilon_N + \varepsilon_p) \\ W_s = 0 & \dfrac{\mathrm{d}^2 W_s}{\mathrm{d}\xi^2} = -\dfrac{1}{2}\varepsilon_M \\ \dfrac{\mathrm{d}W_s}{\mathrm{d}\xi} = 0 & \dfrac{\mathrm{d}^3 W_s}{\mathrm{d}\xi^3} = -\dfrac{1}{2}\varepsilon_Q \end{array}\right\} \tag{26}$$

$$\left.\begin{array}{ll} \xi = 0 : U_a = 0 & \xi = 1 : \dfrac{\mathrm{d}U_a}{\mathrm{d}\xi} = \dfrac{1}{2}(\varepsilon_N - \varepsilon_p) \\ W_a = 0 & \dfrac{\mathrm{d}^2 W_a}{\mathrm{d}\xi^2} = -\dfrac{1}{2}\varepsilon_M \\ \dfrac{\mathrm{d}W_a}{\mathrm{d}\xi} = 0 & \dfrac{\mathrm{d}^3 W_a}{\mathrm{d}\xi^3} = \dfrac{6\tau_n}{E_{nh} r_h^3} - \dfrac{1}{2}\varepsilon_Q \end{array}\right\} \tag{27}$$

In the above equations:

$$\varepsilon_p = \frac{\varepsilon_e}{r_h}, \quad \varepsilon_e = -\frac{e_{31} V_1}{E_h h}, \quad \varepsilon_N = \frac{N_{\mathrm{int}}}{E_{nh} r_h}, \quad \varepsilon_M = \frac{12 M_{\mathrm{int}}}{E_{nh} r_h^3}, \quad \varepsilon_Q = \frac{12 Q_{\mathrm{int}}}{E_{nh} r_h^3} \tag{28}$$

$$\varepsilon_F = \frac{F_{0n}}{E_{nh} r_h}, \quad \varepsilon_P = \frac{12 P_{0n}}{E_h r_h^3} \tag{29}$$

where ε_e is the electrically induced strain of the PZT and V_1 is the magnitude of the applied voltage; N_{int}, M_{int}, and Q_{int} are the amplitudes of non-dimensional internal forces at the intersection between Sections I and II of the host beam; F_{0n} and P_{0n} are the amplitudes of non-dimensional applied forces at the free end of the host beam at which the applied bending moment is assumed to be zero as our numerical results show that the frequency spectra in terms of sensing electric charge caused by the bending moment are similar to ones for the applied shear force.

It can be seen that the problem becomes solving the homogeneous differential equation with the inhomogeneous boundary conditions. Performing proper transformations, we may obtain the inhomogeneous differential equations with the homogeneous boundary conditions (Tiersten, 1969), and then the exact solutions, expressing in forms of the Fourier series normally, are the sum of the particular solutions expanded in a series of characteristic functions by the inhomogeneous excitations and the complementary functions shown in Eqs. (12)–(15), (21)–(23), and (30), (31) given as below. With the increase of time, motions defined by the complementary functions will vanish because of structural damping and the particular solutions or steady state motions of the structure will remain.

Alternatively, we may substitute the inhomogeneous boundary conditions into the complementary functions to find the integration constants and then the steady state solutions are also obtained as follows.

3.2. Solutions of Section II

The dynamic solutions to Section II of the smart beam (Thomson, 1998) are:

$$u_{nh\mathrm{II}} = U_{nh\mathrm{II}}(\xi) \sin \Omega t_n, \quad w_{nh\mathrm{II}} = W_{nh\mathrm{II}}(\xi) \sin \Omega t_n \tag{30}$$

$$\left.\begin{array}{l} U_{nh\mathrm{II}} = A_{h1} \sin \beta_{s1}\xi + A_{h2} \cos \beta_{s1}\xi \\ W_{nh\mathrm{II}} = (B_{h1} \sinh \beta_h \xi + B_{h2} \cosh \beta_h \xi + B_{h3} \sin \beta_h \xi + B_{h4} \cos \beta_h \xi) \\ \text{where, } \beta_h = \sqrt{\dfrac{\omega}{\alpha_w}}. \end{array}\right\} \tag{31}$$

Substituting the boundary conditions of Section II shown in Eq. (24) into Eq. (31), we find:

$$\left.\begin{aligned} U_{nh\mathrm{II}} &= \frac{1}{\beta_{s1}\sin\beta_{s1}\alpha_p}[\varepsilon_N\cos\beta_{s1}(\alpha_p-\xi)-\varepsilon_F\cos\beta_{s1}\xi] \\ W_{nh\mathrm{II}} &= \frac{\Delta_{h1}}{\Delta_h}(\sinh\beta_h\xi+\sin\beta_h\xi)+\frac{\Delta_{h2}}{\Delta_h}(\cosh\beta_h\xi+\cos\beta_h\xi)+\varepsilon_M\frac{\cos\beta_h\xi}{\beta_h^2}+\varepsilon_Q\frac{\sin\beta_h\xi}{\beta_h^3} \end{aligned}\right\} \tag{32}$$

where

$$\left.\begin{aligned} \Delta_{h1} &= \frac{1}{\beta_h^3}[\beta_h\varepsilon_M(\sinh\beta_h\alpha_p\cos\beta_h\alpha_p+\cosh\beta_h\alpha_p\sin\beta_h\alpha_p)+\varepsilon_Q(\sinh\beta_h\alpha_p\sin\beta_h\alpha_p \\ &\quad -\cosh\beta_h\alpha_p\cos\beta_h\alpha_p+1)+\varepsilon_P(\cosh\beta_h\alpha_p-\cos\beta_h\alpha_p)] \\ \Delta_{h2} &= \frac{1}{\beta_h^3}[-\beta_h\varepsilon_M(\sinh\beta_h\alpha_p\sin\beta_h\alpha_p+\cosh\beta_h\alpha_p\cos\beta_h\alpha_p-1)+\varepsilon_Q(\sinh\beta_h\alpha_p\cos\beta_h\alpha_p \\ &\quad -\cosh\beta_h\alpha_p\sin\beta_h\alpha_p)-\varepsilon_P(\sinh\beta_h\alpha_p-\sin\beta_h\alpha_p)] \\ \Delta_h &= 2(\cosh\beta_h\alpha_p\cos\beta_h\alpha_p-1) \end{aligned}\right\} \tag{33}$$

3.3. Solutions of Section I

Substituting the boundary conditions of Section I shown in Eq. (26) into Eqs. (12) and (13), we have:

$$\left.\begin{aligned} U_s &= \frac{\sin\beta_{s1}\xi}{\beta_{s1}\cos\beta_{s1}}\frac{1}{2}(\varepsilon_N+\varepsilon_p) \\ W_s &= \frac{\Delta_{s1}}{\Delta_s}(\sinh\beta_e\xi\sin\beta_e\xi)+\frac{\Delta_{s2}}{\Delta_s}(\cosh\beta_e\xi\sin\beta_e\xi-\sinh\beta_e\xi\cos\beta_e\xi) \end{aligned}\right\} \tag{34}$$

where

$$\left.\begin{aligned} \Delta_{s1} &= \frac{1}{\beta_e^3}\left[2\beta_e\cosh\beta_e\cos\beta_e\left(-\frac{\varepsilon_M}{2}\right)-(\sinh\beta_e\cos\beta_e+\cosh\beta_e\sin\beta_e)\left(-\frac{\varepsilon_Q}{2}\right)\right] \\ \Delta_{s2} &= \frac{1}{\beta_e^3}\left[-\beta_e(\sinh\beta_e\cos\beta_e-\cosh\beta_e\sin\beta_e)\left(-\frac{\varepsilon_M}{2}\right)+\cosh\beta_e\cos\beta_e\left(-\frac{\varepsilon_Q}{2}\right)\right] \\ \Delta_s &= \cosh 2\beta_e+\cos 2\beta_e \end{aligned}\right\} \tag{35}$$

To solve Eq. (21), we firstly derive the relations of A_{ai} and B_{ai} $(i=1,2,\ldots,6)$, which can be obtained by substituting Eq. (21) into the first formulation of Eq. (10):

$$\left.\begin{aligned} A_{a1} &= K_1B_{a2}, \quad A_{a3}=K_2B_{a4}, \quad A_{a5}=K_3B_{a6} \\ A_{a2} &= K_1B_{a1}, \quad A_{a4}=K_2B_{a3}, \quad A_{a6}=-K_3B_{a5} \end{aligned}\right\} \tag{36}$$

where

$$\left.\begin{aligned} K_1 &= \beta_1K_{10}=\frac{r_h}{2}\frac{\beta_1\beta_{au}^2}{\beta_1^2-(\beta_{au}^2-\beta_{\omega u}^2)} \\ K_2 &= \beta_2K_{20}=\frac{r_h}{2}\frac{\beta_2\beta_{au}^2}{\beta_2^2-(\beta_{au}^2-\beta_{\omega u}^2)} \\ K_3 &= \beta_3K_{30}=\frac{r_h}{2}\frac{\beta_3\beta_{au}^2}{\beta_3^2+(\beta_{au}^2-\beta_{\omega u}^2)} \end{aligned}\right\} \tag{37}$$

Substituting the boundary conditions at $\xi=0$ shown in Eq. (27) into Eq. (21), and considering the relations shown in Eq. (36), we have:

$$\left.\begin{aligned} U_a &= B_{a2}(K_1\sinh\beta_1\xi - K_3\sin\beta_3\xi) + B_{a4}(K_2\sinh\beta_2\xi - K_3\sin\beta_3\xi) \\ &\quad + B_{a5}(K_1K_{31}\cosh\beta_1\xi + K_2K_{32}\cosh\beta_2\xi - K_3\cos\beta_3\xi) \\ W_a &= B_{a2}(\cosh\beta_1\xi - \cos\beta_3\xi) + B_{a4}(\cosh\beta_2\xi - \cos\beta_3\xi) \\ &\quad + B_{a5}(K_{31}\sinh\beta_1\xi + K_{32}\sinh\beta_2\xi + \sin\beta_3\xi) \end{aligned}\right\} \tag{38}$$

where

$$K_{31} = \frac{\beta_3(K_{30}+K_{20})}{\beta_1(K_{10}-K_{20})}, \quad K_{32} = \frac{\beta_3(K_{30}+K_{10})}{\beta_2(K_{20}-K_{10})} \tag{39}$$

Considering the boundary conditions at $\xi = 1$ and the expression of the shear stress shown in Eq. (9), we can obtain the equations for solving the integration constants B_{a2}, B_{a4} and B_{a5}, in which the unknown internal forces of the host beam at the intersection are included:

$$\left.\begin{aligned} &B_{a2}(\beta_1^2K_{10}\cosh\beta_1 - \beta_3^2K_{30}\cos\beta_3) + B_{a4}(\beta_2^2K_{20}\cosh\beta_2 - \beta_3^2K_{30}\cos\beta_3) \\ &\quad + B_{a5}(\beta_1^2K_{10}K_{31}\sinh\beta_1 + \beta_2^2K_{20}K_{32}\sinh\beta_2 + \beta_3^2K_{30}\sin\beta_3) = \frac{\varepsilon_N - \varepsilon_p}{2} \\ &B_{a2}(\beta_1^2\cosh\beta_1 + \beta_3^2\cos\beta_3) + B_{a4}(\beta_2^2\cosh\beta_2 + \beta_3^2\cos\beta_3) \\ &\quad + B_{a5}(\beta_1^2K_{31}\sinh\beta_1 + \beta_2^2K_{32}\sinh\beta_2 - \beta_3^2\sin\beta_3) = -\frac{\varepsilon_M}{2} \\ &B_{a2}(K_{\beta1}\sinh\beta_1 - K_{\beta3}\sin\beta_3) + B_{a4}(K_{\beta2}\sinh\beta_2 - K_{\beta3}\sin\beta_3) \\ &\quad + B_{a5}(K_{\beta1}K_{31}\cosh\beta_1 + K_{\beta2}K_{32}\cosh\beta_2 - K_{\beta3}\cos\beta_3) = -\frac{\varepsilon_Q}{2} \end{aligned}\right\} \tag{40}$$

where

$$\left.\begin{aligned} K_{\beta1} &= \beta_1\left[\beta_1^2 - \frac{12r_{\tau a}}{E_{nh}r_h^3}\left(K_{10} + \frac{r_h}{2}\right)\right] \\ K_{\beta2} &= \beta_2\left[\beta_2^2 - \frac{12r_{\tau a}}{E_{nh}r_h^3}\left(K_{20} + \frac{r_h}{2}\right)\right] \\ K_{\beta3} &= \beta_3\left[\beta_3^2 - \frac{12r_{\tau a}}{E_{nh}r_h^3}\left(K_{30} - \frac{r_h}{2}\right)\right] \end{aligned}\right\} \tag{41}$$

Integration constants B_{a2}, B_{a4} and B_{a5} are solved by Eq. (40):

$$\left.\begin{aligned} B_{a2} &= \frac{1}{\Delta_a}\left[\Delta_{N2}\frac{\varepsilon_N - \varepsilon_p}{2} + \Delta_{M2}\left(-\frac{\varepsilon_M}{2}\right) + \Delta_{Q2}\left(-\frac{\varepsilon_Q}{2}\right)\right] \\ B_{a4} &= \frac{1}{\Delta_a}\left[\Delta_{N4}\frac{\varepsilon_N - \varepsilon_p}{2} + \Delta_{M4}\left(-\frac{\varepsilon_M}{2}\right) + \Delta_{Q4}\left(-\frac{\varepsilon_Q}{2}\right)\right] \\ B_{a5} &= \frac{1}{\Delta_a}\left[\Delta_{N5}\frac{\varepsilon_N - \varepsilon_p}{2} + \Delta_{M5}\left(-\frac{\varepsilon_M}{2}\right) + \Delta_{Q5}\left(-\frac{\varepsilon_Q}{2}\right)\right] \end{aligned}\right\} \tag{42}$$

where Δ_a is the determinant value of the coefficient matrix of Eq. (40) and Δ_{Nk} $(N = N, M, Q; k = 2, 4, 5)$ are determinant values of the corresponding cofactors.

3.4. Exact dynamic solutions of the smart beam

The motion equations of the smart beam we have solved still include the unknown internal forces of the host beam at the intersection. To determine the unknowns, we consider the continuity and smooth conditions at the intersection:

$$U_{nh}(1) = U_{nh\mathrm{II}}(0), \quad W_{nh}(1) = W_{nh\mathrm{II}}(0), \quad \frac{\mathrm{d}W_{nh}(1)}{\mathrm{d}\xi} = \frac{\mathrm{d}W_{nh\mathrm{II}}(0)}{\mathrm{d}\xi} \tag{43}$$

where

$$U_{nh}(1) = U_a(1) + U_s(1), \quad W_{nh}(1) = W_a(1) + W_s(1), \quad \frac{\mathrm{d}W_{nh}(1)}{\mathrm{d}\xi} = \frac{\mathrm{d}W_a(1)}{\mathrm{d}\xi} + \frac{\mathrm{d}W_s(1)}{\mathrm{d}\xi} \tag{44}$$

The expressions of the intersectional displacements can be found by Eqs. (32), (34) and (38), which are given in Appendix B. Substituting Eqs. (B.1)–(B.3) into the continuity and smooth equations (43), we have:

$$\left.\begin{aligned} b_{11}\varepsilon_N + b_{12}\varepsilon_M + b_{13}\varepsilon_Q &= c_{1e}\varepsilon_p + c_{1F}\varepsilon_F \\ b_{21}\varepsilon_N + b_{22}\varepsilon_M + b_{23}\varepsilon_Q &= c_{2e}\varepsilon_p + c_{2P}\varepsilon_P \\ b_{31}\varepsilon_N + b_{32}\varepsilon_M + b_{33}\varepsilon_Q &= c_{3e}\varepsilon_p + c_{3P}\varepsilon_P \end{aligned}\right\} \tag{45}$$

The coefficients in Eq. (45) are given in Appendix B.

The unknown forces at the intersection can be solved by Eq. (45). By substituting the solved unknown forces into Eqs. (32), (34) and (38), the integration constants are determined, and therefore the steady state motions of the smart beam are found.

We have mentioned that the proper transformations may be constructed to change the problem of homogeneous differential equations with the inhomogeneous boundary conditions into that of inhomogeneous differential equations with the homogeneous boundary conditions. In doing so, by having the coefficients of characteristic functions be unlimited, the natural frequencies are obtained, and the characteristic functions are the normal mode shapes.

Based on the solved steady state motions, the frequency spectra can be easily plotted. When the frequency approaches to the resonant frequency, the solution is divergent and thus the natural frequency is found. The mode shape of each order can be accurately obtained by selecting the frequency very close to the resonant frequency.

3.5. Exact dynamic solutions tailored to a bimorph bender

The obtained solutions of the cantilever beam with a partially bonded PZT patch to the fixed end can be tailored to directly solve the PZT double cantilever beam (DCB). When the DCB undergoes pure bending deformation, it is a PZT bimorph bender, which has been widely used in the area of micro-controls. The boundary conditions of the DCB can be expressed:

$$\left.\begin{aligned} \xi = 0 : U_s = 0 \qquad & \xi = 1 : \frac{\mathrm{d}U_s}{\mathrm{d}\xi} = \varepsilon_{Ns} + \varepsilon_{ps} = \frac{1}{2}(\varepsilon_{Nh} + \varepsilon_{N1} + \varepsilon_{ph} + \varepsilon_{p1}) \\ W_s = 0 \qquad & \frac{\mathrm{d}^2 W_s}{\mathrm{d}\xi^2} = -\varepsilon_{Ms} = -\frac{1}{2}(\varepsilon_{Mh} - \varepsilon_{M1}) \\ \frac{\mathrm{d}W_s}{\mathrm{d}\xi} = 0 \qquad & \frac{d^3 W_s}{d\xi^3} = -\varepsilon_{Qs} = -\frac{1}{2}(\varepsilon_{Qh} - \varepsilon_{Q1}) \end{aligned}\right\} \tag{46}$$

$$\left.\begin{aligned} \xi = 0 : U_a = 0 \qquad & \xi = 1 : \frac{\mathrm{d}U_a}{\mathrm{d}\xi} = \varepsilon_{Na} + \varepsilon_{pa} = \frac{1}{2}(\varepsilon_{Nh} - \varepsilon_{N1} + \varepsilon_{ph} - \varepsilon_{p1}) \\ W_a = 0 \qquad & \frac{\mathrm{d}^2 W_a}{\mathrm{d}\xi^2} = -\varepsilon_{Ma} = -\frac{1}{2}(\varepsilon_{Mh} + \varepsilon_{M1}) \\ \frac{\mathrm{d}W_a}{\mathrm{d}\xi} = 0 \qquad & \frac{\mathrm{d}^3 W_a}{\mathrm{d}\xi^3} - \frac{6\tau_n}{E_h r_h^3} = -\varepsilon_{Qa} = -\frac{1}{2}(\varepsilon_{Qh} + \varepsilon_{Q1}) \end{aligned}\right\} \tag{47}$$

In the above equations:

$$\varepsilon_{pk}=\frac{\varepsilon_{ek}}{r_h},\quad \varepsilon_{Nk}=\frac{N_{nk}}{E_{nh}r_h},\quad \varepsilon_{Mk}=\frac{12M_{nk}}{E_{nh}r_h^3},\quad \varepsilon_{Qk}=\frac{12Q_{nk}}{E_{nh}r_h^3},\quad (k=s,a,1,h) \tag{48}$$

where ε_{ek} is the induced strain; N_{nk}, M_{nk} and Q_{nk} $(k=s,a,1,h)$ are the amplitudes of non-dimensional applied axial forces, bending moments and the shear forces at the free ends.

Substituting Eqs. (46) and (47) into Eqs. (35) and (40) respectively, we have the DCB dynamic solutions shown in Eqs. (34) and (38). When the pure bending deformation is considered, they become the solutions of a bimorph bender.

In the static state of the DCB, dynamic equations (7)–(10) are simplified into the following related equilibrium equations and constitutive relations:

$$N_s=E_{nh}r_h\frac{\mathrm{d}u_s}{\mathrm{d}\xi}+\frac{e_{31}V_s}{G_ah},\quad M_s=-\frac{E_{nh}r_h^3}{12}\frac{\mathrm{d}^2w_s}{\mathrm{d}\xi^2},\quad \sigma_n=2r_{\sigma a}w_s \tag{49}$$

$$\left.\begin{aligned}&E_{nh}r_h^2\frac{\mathrm{d}^2u_s}{\mathrm{d}\xi^2}=0\\&-\frac{E_{nh}r_h^4}{12}\frac{\mathrm{d}^4w_s}{\mathrm{d}\xi^4}-2r_{\sigma a}w_s=0\end{aligned}\right\} \tag{50}$$

$$N_a=E_{nh}r_h\frac{\mathrm{d}u_a}{\mathrm{d}\xi}+\frac{e_{31}V_a}{G_ah},\quad M_a=-\frac{E_{nh}r_h^3}{12}\frac{\mathrm{d}^2w_a}{\mathrm{d}\xi^2},\quad \tau_n=2r_{\tau a}\left(u_a+\frac{r_h}{2}\frac{\mathrm{d}w_a}{\mathrm{d}\xi}\right) \tag{51}$$

$$\left.\begin{aligned}&E_{nh}r_h^2\frac{\mathrm{d}^2u_a}{\mathrm{d}\xi^2}-2r_{\tau a}\left(u_a\frac{r_h}{2}\frac{\mathrm{d}w_a}{\mathrm{d}\xi}\right)=0\\&-\frac{E_{nh}r_h^4}{12}\frac{\mathrm{d}^4w_a}{\mathrm{d}\xi^4}+2r_{\tau a}\frac{r_h}{2}\left(\frac{\mathrm{d}u_a}{\mathrm{d}\xi}+\frac{r_h}{2}\frac{\mathrm{d}^2w_a}{\mathrm{d}\xi^2}\right)=0\end{aligned}\right\} \tag{52}$$

By integrating differential equations (49) and (50) with the boundary conditions given in Eq. (46), the solutions of u_s, w_s and σ_n are given by:

$$\left.\begin{aligned}&u_s=(\varepsilon_{Ns}+\varepsilon_{ps})\xi\\&w_s=B_{ss1}\sinh\beta_{es}\xi\sin\beta_{es}\xi+B_{ss2}(\cosh\beta_{es}\xi\sin\beta_{es}\xi-\sinh\beta_{es}\xi\cos\beta_{es}\xi)\\&\sigma_n=2r_{\sigma a}w_s\end{aligned}\right\} \tag{53}$$

where

$$\left.\begin{aligned}&\beta_\sigma=\sqrt[4]{\frac{24r_{\sigma a}}{E_{nh}r_h^4}},\quad \beta_{es}=\frac{\sqrt{2}}{2}\beta_\sigma\\&B_{ss1}=\frac{-2\beta_{es}\varepsilon_{Ms}\cosh\beta_{es}\cos\beta_{es}+\varepsilon_{Qs}(\sinh\beta_{es}\cos\beta_{es}+\cosh\beta_{es}\sin\beta_{es})}{\beta_{es}^3(\cosh2\beta_{es}+\cos2\beta_{es})}\\&B_{ss2}=\frac{\beta_{es}\varepsilon_{Ms}(\sinh\beta_{es}\cos\beta_{es}-\cosh\beta_{es}\sin\beta_{es})-\varepsilon_{Qs}\cosh\beta_{es}\cos\beta_{es}}{\beta_{es}^3(\cosh2\beta_{es}+\cos2\beta_{es})}\end{aligned}\right\} \tag{54}$$

The non-dimensional shear stress can be determined by solving the differential equations (51) and (52) with the boundary conditions expressed as:

$$\left.\begin{aligned}&\xi=0:\tau_n=0\\&\xi=1:\frac{\mathrm{d}\tau_n}{\mathrm{d}\xi}=2r_{\tau a}\left(\varepsilon_{Na}+\varepsilon_{ea}-\frac{r_h}{2}\varepsilon_{Ma}\right),\quad \frac{\mathrm{d}^2\tau_n}{\mathrm{d}\xi^2}-\beta_\tau^2\tau_n=-r_hr_{\tau a}\varepsilon_{Qa}\end{aligned}\right\} \tag{55}$$

The non-dimensional shear stress is then found to be:

$$\tau_n = (A_{Ne1} + A_{M1} + A_{Q1}) \sinh \beta_\tau \xi + A_{Q2}(\cosh \beta_\tau \xi - 1) \tag{56}$$

where

$$\left.\begin{aligned} &\beta_\tau = \sqrt{2r_{\tau a}\left(\frac{1}{E_{nh}r_h^2} + \frac{3}{E_{nh}r_h^2}\right)} = \sqrt{\frac{8r_{\tau a}}{E_{nh}r_h^2}} \\ &A_{Ne1} = \frac{2r_{\tau a}(\varepsilon_{Na} + \varepsilon_{pa})}{\beta_\tau \cosh \beta_\tau}, \quad A_{M1} = -\frac{r_h r_{\tau a}\varepsilon_{Ma}}{\beta_\tau \cosh \beta_\tau} \\ &A_{Q1} = \frac{r_h r_{\tau a}\varepsilon_{Qa}}{\beta_\tau^2} th\beta_e, \quad A_{Q2} = -\frac{r_h r_{\tau a}\varepsilon_{Qa}}{\beta_\tau^2} \end{aligned}\right\} \tag{57}$$

For the PZT bimorph bender, only the solutions of Eqs. (51) and (52) need to be considered. In this case, the actuated forces in one of the PZTs, e.g., in the one referred to as the host beam, can be found by utilizing the equilibrium equations, and they are given by:

$$N_{nh} = \frac{1}{\beta_\tau}(A_{Ne1} + A_{M1} + A_{Q1})(\cosh \beta_\tau \xi - \cosh \beta_\tau) + \frac{1}{\beta_\tau} A_{Q2}(\sinh \beta_\tau \xi - \sinh \beta_\tau) + A_{Q2}(\xi - 1) \tag{58}$$

$$M_{nh} = -\frac{1}{2}\left[\frac{1}{\beta_\tau}(A_{Ne1} + A_{M1} + A_{Q1})(\cosh \beta_\tau \xi - \cosh \beta_\tau) + \frac{1}{\beta_\tau} A_{Q2}(\sinh \beta_\tau \xi - \sinh \beta_\tau) + A_{Q2}(\xi - 1)\right] \tag{59}$$

As the shear stress concentration occurs at the free end, the actuated axial force and bending moment attain their asymptotes in the region distant from the free end. It can also be shown that, the equivalent actuated forces obtained in Part II of the exact static solutions (Luo and Tong, 2002a,b) are very close to the maximum values given in Eqs. (58) and (59). The equivalent forces in dimensional form are:

$$N_{eq} = \frac{Eh}{8}\varepsilon_{ea}, \quad M_{eq} = \frac{Eh^2}{16}\varepsilon_{ea} \tag{60}$$

Using the *Euler–Bernoulli* beam theory (Timoshenko and Gere, 1972), we can easily derive the actuated rotation angle and deflection at the free end and thus the relations between the angle or deflection and the voltage are:

$$k_{14} = k_{41} = \frac{3e_{31}L_p}{4Eh^2}, \quad k_{24} = k_{42} = \frac{3e_{31}L_p^2}{8Eh^2} \tag{61}$$

The relations given in Eq. (61) are the same as those formulated by Smits et al. (1991) and Wang and Cross (1999). The other matched components in the constitutive relation matrix can also be derived using the same procedures.

4. Exact solutions of the shear lag models

Crawley and de Luis (1987) developed a shear lag model for a smart beam, in which the PZT patches were modeled as rods; the finite thickness adhesive was assumed to transfer shear stresses only, and the host beam was assumed to deform in extension or in pure bending only. Im and Atluri (1989) extended this static model to account for a more general state of external loadings on the host beam. Crawley and Anderson (1990) compared two analytical models of the static interaction between a host beam and the symmetrically bonded PZT actuators. The second model was a refinement of the first one developed by Crawley and

de Luis (1987), which accounted for both extension and bending of both the PZT patches and the host beam while retaining the assumption of the pure shear stress state in the adhesive.

Crawley and de Luis (1987) investigated the dynamic influence of the piezoelectric actuators using the shear stress derived from the static analysis as the exciting function, or based on the equivalent forces. On the basis of their equivalent forces obtained through the extended static analysis, Crawley and Anderson (1990) also conducted the dynamic analysis using their two models and similar results were obtained for the case when the PZT patches are much thinner than the host beam; Im and Atluri (1989) also formulated their equivalent forces, which were also used for investigating dynamic controls (Shi and Atluri, 1990).

We have derived the exact dynamic solutions for PZT smart beams including peel stresses. In our static analysis (Luo and Tong, 2002a,b), it was shown that the finite thickness adhesive with the shear and peel stresses provided more accurate results, especially for the flexible structures; the errors predicted by the shear lag model may be as high as up to 90%. In the dynamic analysis, we will also compare the present dynamic model including peel stresses (PSM) with the shear lag model. To do so, we first derive the exact dynamic solutions for the dynamic model with only the shear stress in the adhesive layer.

Two dynamic models, referred to as a shear lag rod model (SLRM) and shear lag beam model (SLBM), are presented for the smart beam shown in Fig. 1 in this section, and the exact dynamic solutions to a smart beam with different substrates will be derived in Appendix A. The present exact solutions to shear lag models are different from the approximate solutions given by Crawley and de Luis (1987), and Crawley and Anderson (1990). Motions of PZT patches are considered in our formulations.

4.1. Shear lag beam model

In Eqs. (2)–(7), setting $\sigma_n = 0$, we can obtain the related equations for the shear lag beam model. Eq. (8) becomes:

$$\left.\begin{aligned} E_{nh} r_h^2 \frac{\partial^2 u_{sb}}{\partial \xi^2} &= m_n \frac{\partial^2 u_{sb}}{\partial t_n^2} \\ -\frac{E_{nh} r_h^4}{12} \frac{\partial^4 w_{sb}}{\partial \xi^4} &= m_n \frac{\partial^2 w_{sb}}{\partial t_n^2} \end{aligned}\right\} \tag{62}$$

Eqs. (9) and (10) and the solutions are the same as those of the present model including peel stresses. Solutions to Eq. (62) are:

$$\left.\begin{aligned} U_{sb} &= A_{sb1} \sin \beta_{s1} \xi + A_{sb2} \cos \beta_{s1} \\ W_{sb} &= (B_{sb1} \sinh \beta_h \xi + B_{sb2} \cosh \beta_h \xi + B_{sb3} \sin \beta_h \xi + B_{sb4} \cos \beta_h \xi) \end{aligned}\right\} \tag{63}$$

Substituting the boundary conditions shown in Eq. (26) into (63), we have:

$$\left.\begin{aligned} U_{sb} &= \frac{\sin \beta_{s1} \xi}{\beta_{s1} \cos \beta_{s1}} \frac{1}{2} (\varepsilon_N + \varepsilon_p) \\ W_{sb} &= \frac{\Delta_{sb1}}{\Delta_{sb}} (\sinh \beta_h \xi - \sin \beta_h \xi) + \frac{\Delta_{sb2}}{\Delta_{sb}} (\cosh \beta_h \xi - \cos \beta_h \xi) \end{aligned}\right\} \tag{64}$$

where

$$\left.\begin{aligned} \Delta_{sb} &= 2(\cosh \beta_h \cos \beta_h + 1) \\ \Delta_{sb1} &= \frac{1}{\beta_h^3} \Big[-\beta_h (\sinh \beta_h - \sin \beta_h) \Big(-\frac{\varepsilon_M}{2} \Big) + (\cosh \beta_h + \cos \beta_h) \Big(-\frac{\varepsilon_Q}{2} \Big) \Big] \\ \Delta_{sb2} &= \frac{1}{\beta_h^3} \Big[\beta_h (\cosh \beta_h + \cos \beta_h) \Big(-\frac{\varepsilon_M}{2} \Big) - (\sinh \beta_h + \sin \beta_h) \Big(-\frac{\varepsilon_Q}{2} \Big) \Big] \end{aligned}\right\} \tag{65}$$

At the intersection between Sections I and II of the host beam, $U_{sb}(1)$ is the same as that of PSM. The deflection and the related slope are:

$$\left.\begin{aligned} W_{sb}(1) &= -\frac{\varepsilon_M\beta_h\sinh\beta_h\sin\beta_h+\varepsilon_Q(\sinh\beta_h\cos\beta_h-\cosh\beta_h\sin\beta_h)}{2\beta_h^3(\cosh\beta_h\cos\beta_h+1)} \\ \frac{\mathrm{d}W_{sb}(1)}{\mathrm{d}\xi} &= \frac{-\varepsilon_M\beta_h(\sinh\beta_h\cos\beta_h+\cosh\beta_h\sin\beta_h)+\varepsilon_Q\sinh\beta_h\sin\beta_h}{2\beta_h^2(\cosh\beta_h\cos\beta_h+1)} \end{aligned}\right\} \tag{66}$$

Replacing the related items of b_{22}, b_{23}, b_{32} and b_{33} in Eqs. (B.8) and (B.9) with the derived expressions shown in Eq. (66), we have the equation with the same form as that of Eq. (45), and then the unknown forces at the intersection between Sections I and II are solved. Substituting the obtained forces at the intersection into Eqs. (32), (64) and (38), we find the steady state motions for the shear lag beam model, and the numerical comparisons will be presented in Part II of this work.

We can show that, except for the area near the free PZT edge, the peel stress predicted by the present model is almost zero, and thus that $w_{nh}=w_{n1}$ holds true in the area distant to the PZT edge. However, the shear lag beam model gives:

$$w_{nh}=w_{n1}+\left[\frac{\Delta_{sb1}}{\Delta_{sb}}(\sinh\beta_h\xi-\sin\beta_h\xi)+\frac{\Delta_{sb2}}{\Delta_{sb}}(\cosh\beta_h\xi-\cos\beta_h\xi)\right]\sin\Omega t_n \tag{67}$$

The relation of $w_{nh}=w_{n1}$ is true only in static state.

4.2. Shear lag rod model

The formulation procedures for SLRM are similar to those of PSM. Only the equations that are different from those of the previous formulation are given. In SLRM, Eqs. (2) and (3) are simplified as follows:

$$\left.\begin{aligned} &r_h\frac{\partial N_{n1}}{\partial\xi}+\tau_n=m_n\frac{\partial^2u_{n1}}{\partial t_n^2} \\ &r_h\frac{\partial N_{nh}}{\partial\xi}-\tau_n=m_n\frac{\partial^2u_{nh}}{\partial t_n^2},\quad r_h\frac{\partial Q_{nh}}{\partial\xi}=m_n\frac{\partial^2w_{nh}}{\partial t_n^2},\quad \frac{\partial M_{nh}}{\partial\xi}+\frac{1}{2}\tau_n-Q_{nh}=0 \end{aligned}\right\} \tag{68}$$

The constitutive equation of the adhesive is given by:

$$\tau_n=r_{\tau a}\left[(u_{nh}-u_{n1})+\frac{r_h}{2}\frac{\partial w_{nh}}{\partial\xi}\right] \tag{69}$$

The motion equations can be simplified as:

$$\left.\begin{aligned} &E_{nh}r_h^2\frac{\partial^2u_{n1}}{\partial\xi^2}+r_{\tau a}\left[(u_{nh}-u_{n1})+\frac{r_h}{2}\frac{\partial w_{nh}}{\partial\xi}\right]=m_n\frac{\partial^2u_{n1}}{\partial t_n^2} \\ &E_{nh}r_h^2\frac{\partial^2u_{nh}}{\partial\xi^2}-r_{\tau a}\left[(u_{nh}-u_{n1})+\frac{r_h}{2}\frac{\partial w_{nh}}{\partial\xi}\right]=m_n\frac{\partial^2u_{nh}}{\partial t_n^2} \\ &-\frac{E_{nh}r_h^4}{12}\frac{\partial^4w_{nh}}{\partial\xi^4}+\frac{r_{\tau a}r_h}{2}\left[\left(\frac{\partial u_{nh}}{\partial\xi}-\frac{\partial u_{n1}}{\partial\xi}\right)+\frac{r_h}{2}\frac{\partial^2w_{nh}}{\partial\xi^2}\right]=m_n\frac{\partial^2w_{nh}}{\partial t_n^2} \end{aligned}\right\} \tag{70}$$

Eqs. (8) and (10) become:

$$E_{nh}r_h^2\frac{\partial^2u_{sr}}{\partial\xi^2}=m_n\frac{\partial^2u_{sr}}{\partial t_n^2} \tag{71}$$

$$\left.\begin{aligned} &E_{nh}r_h^2\frac{\partial^2 u_{ar}}{\partial\xi^2}-2r_{\tau a}\left(u_{ar}+\frac{r_h}{2}\frac{\partial w_{ar}}{\partial\xi}\right)=m_n\frac{\partial^2 u_{ar}}{\partial t_n^2}\\ &-\frac{E_{nh}r_h^4}{12}\frac{\partial^4 w_{ar}}{\partial\xi^4}+2r_{\tau a}\frac{r_h}{4}\left(\frac{\partial u_{ar}}{\partial\xi}+\frac{r_h}{2}\frac{\partial^2 w_{ar}}{\partial\xi^2}\right)=m_n\frac{\partial^2 w_{ar}}{\partial t_n^2}\end{aligned}\right\} \tag{72}$$

It is noted that, $2Q_{ar}=Q_{nh}$, $2M_{ar}=M_{nh}$ and $2w_{ar}=w_{nh}$ in this case.

The characteristic equation (18) can be rewritten as:

$$\left.\begin{aligned} &[\alpha_u^2\beta^2+(\omega^2-\alpha_a^2)]A_a-\frac{r_h}{2}\beta\alpha_a^2B_a=0\\ &\frac{r_h}{4}\beta\alpha_a^2A_a-\left[\alpha_w^2\beta^4-\left(\frac{r_h^2}{8}\alpha_a^2\beta^2+\omega^2\right)\right]B_a=0\end{aligned}\right\} \tag{73}$$

The condition for obtaining non-trivial solutions of A_a and B_a is the same as that of the characteristic equation (19) and the other formulations are also similar to the previous demonstrations, except for:

$$\left.\begin{aligned} &\beta_{aw}=\frac{\sqrt{2}r_h\alpha_a}{4\alpha_w}\\ &K_{\beta sri}=\beta_{sri}\left[\beta_{sri}^2-\frac{6r_{\tau a}}{E_{nh}r_h^3}\left(K_{i0}+\frac{r_h}{2}\right)\right]\ (i=1,2),\quad K_{\beta sr3}=\beta_{sr3}\left[\beta_{sr3}^2-\frac{6r_{\tau a}}{E_{nh}r_h^3}\left(K_{30}-\frac{r_h}{2}\right)\right]\end{aligned}\right\} \tag{74}$$

As β_{aw} for SLRM is different, the eigenvalues β_{sri} $(i=1,2,3)$ evaluated from Eq. (19) are different from those of PSM. Using the same procedure, we can solve U_{sr}, U_{ar} and W_{ar}, which are expressed in forms of Eqs. (34) and (38), except for replacing β_i with β_{sri} $(i=1,2,3)$ respectively.

At the intersection between Sections I and II of the host beam,

$$W_{nh}(1)=2W_{ar}(1),\quad \frac{\mathrm{d}W_{nh}(1)}{\mathrm{d}\xi}=2\frac{\mathrm{d}W_{ar}(1)}{\mathrm{d}\xi} \tag{75}$$

The intersectional forces can still be found by using Eq. (45), except for setting W_{sr} to be zero in Eqs. (B.7)–(B.12). Substituting the found intersectional forces into Eqs. (32), (34) and (38), we can obtain the exact solutions to the shear lag rod model.

Following the similar method, dynamic solutions of the composite beam with different materials and geometric parameters can be analytically solved for the shear lag rod model, which are given in Appendix A.

5. Discussion

Using the same solution procedure, Eqs. (14), (15), (22) and (23) can also be solved, and then the exact solutions related to very high frequency for the model of Fig. 1 are obtained. Due to space limitation, they are not given in details here.

In Eq. (19), when $\omega=\alpha_a$, or $(\beta_{au}^2-\beta_{\omega u}^2)=0$, it becomes:

$$\lambda^2-[\beta_{aw}^2+(\beta_{au}^2-\beta_{\omega u}^2)]\lambda-(\beta_{\omega w}^2+\beta_{aw}^2\beta_{\omega u}^2)=0 \tag{76}$$

The roots of Eq. (76) are explicitly given as:

$$\lambda_{1,2}=\frac{1}{2}\left\{[\beta_{aw}^2+(\beta_{au}^2-\beta_{\omega u}^2)]\pm\sqrt{[\beta_{aw}^2+(\beta_{au}^2-\beta_{\omega u}^2)]^2+4(\beta_{\omega w}^2+\beta_{aw}^2\beta_{\omega u}^2)}\right\} \tag{77}$$

Noting that,

$$\sqrt{[\beta_{aw}^2 + (\beta_{au}^2 - \beta_{\omega u}^2)]^2 + 4(\beta_{\omega w}^2 + \beta_{aw}^2\beta_{\omega u}^2)} > [\beta_{aw}^2 + (\beta_{au}^2 - \beta_{\omega u}^2)] \tag{78}$$

It is evident that one root of Eq. (76) is positive real number and the other one negative real number. Therefore, the solution can be expressed as given in Eq. (22).

There is at least one real number in Eq. (19). If the other two roots were conjugate complex numbers, the structural vibrations would not be excited. It is drawn that three roots of Eq. (19) are all real numbers, and thus the equation can be rewritten as:

$$(\lambda - \lambda_1)(\lambda - \lambda_2)(\lambda - \lambda_3) = 0, \quad \text{or} \quad \lambda^3 - (\lambda_1 + \lambda_2 + \lambda_3)\lambda^2 + (\lambda_1\lambda_2 + \lambda_2\lambda_3 + \lambda_3\lambda_1)\lambda - \lambda_1\lambda_2\lambda_3 = 0 \tag{79}$$

By comparing Eq. (19) with (79), we have the following formulations.

1. $\lambda_1 > 0$:
   (a) When $\omega < \alpha_a$, $\lambda_2\lambda_3 < 0$; one of roots λ_2 and λ_3 is positive and the other negative.
   (b) When $\omega > \alpha_a$, $\lambda_2\lambda_3 > 0$; either both roots λ_2 and λ_3 are positive or both negative. If both roots are positive, there will be no vibration. Therefore, both roots are negative.
2. $\lambda_1 < 0$:
   (a) When $\omega < \alpha_a$, $\lambda_2\lambda_3 > 0$; either both roots λ_2 and λ_3 are positive or both negative. If both roots are negative, there will be a contradiction to the solutions given in Eq. (22). Therefore, both roots are positive.
   (b) When $\omega > \alpha_a$, $\lambda_2\lambda_3 < 0$; one of roots λ_2 and λ_3 is positive and the other negative.

In summary, when $\omega < \alpha_a$, there are two positive roots and one negative root for the characteristic equation (19), shown in cases 1(a) and 2(a), and the solutions are given by Eq. (21).

When $\omega > \alpha_a$, there are two negative roots and one positive root, shown in cases 1(b) and 2(b), and the solutions are given by Eq. (23).

6. Conclusion

On the basis of the *Euler–Bernoulli* beam theory, piezoelectric relations and the model of adhesive joints developed by Goland and Reissner (1944), the partial differential forms of the motion equations of the smart beam are derived. The partial differential equations are then dissolved into two independent groups of symmetric and anti-symmetric equations using the proper transformation, and then the exact dynamic solutions to piezoelectric smart beams including peel stresses are analytically obtained by assuming the harmonic motions. The exact solutions are applied to the cantilever beam with a bonded PZT patch to the clamped end, whose frequency spectra, resonant frequencies, normal mode shapes, and harmonic responses of the shear and peel stresses can be investigated. Dynamic solutions of the PZT bimorph bender are also discussed briefly, and the constitutive relations derived for the applied voltage agree with the existing expressions.

Acknowledgement

The authors are grateful to the support of Australian Research Council through a Large Grant Scheme (grant no. A10009074).

Appendix A. Exact dynamic solutions for the PZT smart beam with different adherends using the shear lag rod model

The material properties for both the PZT patches and the host beam are still assumed to be the same, whereas the assumption of same geometry is abandoned.

In addition to the non-dimensional parameters defined in Eq. (1), the following parameters are introduced:

$$r_1 = \frac{t_1}{L_p}, \quad m_{n1} = m_{T1}\omega_T^2, \quad m_{T1} = \frac{m_1 h}{G_a} \tag{A.1}$$

where t_1 is the thickness of the PZT patch, m_1 $(= \rho t_1)$ is the density of the PZT patch, mass per unit length. It can be derived that:

$$m_{n1} = \frac{r_1}{r_h} m_n = \frac{1}{R_{ht}} m_n \tag{A.2}$$

where R_{ht} is the thickness ratio of the host beam to the PZT patch.

A.1. A host beam with one bonded PZT patch

As shown in Fig. 3, the PZT dynamic equation is:

$$r_h \frac{\partial N_{n1}}{\partial \xi} + \tau_n = m_{n1} \frac{\partial^2 u_{n1}}{\partial t_n^2} \tag{A.3}$$

The constitutive relation is given by:

$$N_{n1} = E_{nh} r_1 \frac{\partial u_{n1}}{\partial \xi} + \frac{e_{31} V_1(t)}{G_a h} \tag{A.4}$$

The dynamic equations of the host beam and the constitutive relations of the adhesive are the same as those given in Eqs. (68) and (69).

The second and third formulations of Eq. (70) are not changed and the first one of Eq. (70) becomes:

$$E_{nh} r_h r_1 \frac{\partial^2 u_{n1}}{\partial \xi^2} + r_{\tau a}\left[(u_{nh} - u_{n1}) + \frac{r_h}{2}\frac{\partial w_{nh}}{\partial \xi}\right] = \frac{r_1}{r_h} m_n \frac{\partial^2 u_{n1}}{\partial t_n^2} \tag{A.5}$$

The motion equations corresponding to Eqs. (71) and (72) can be derived:

$$E_{nh} r_h^2 \frac{\partial^2 u_{sr}}{\partial \xi^2} = m_n \frac{\partial^2 u_{sr}}{\partial t_n^2} \tag{A.6}$$

$$\left.\begin{aligned} &E_{nh} r_h^2 \frac{\partial^2 u_{ar}}{\partial \xi^2} - r_{\tau a}(1 + R_{ht})\left(u_{ar} + \frac{r_h}{2}\frac{\partial w_{ar}}{\partial \xi}\right) = m_n \frac{\partial^2 u_{ar}}{\partial t_n^2} \\ &-\frac{E_{nh} r_h^4}{12}\frac{\partial^4 w_{ar}}{\partial \xi^4} + r_{\tau a}(1 + R_{ht})\frac{r_h}{2(1 + R_{ht})}\left(\frac{\partial u_{ar}}{\partial \xi} + \frac{r_h}{2}\frac{\partial^2 w_{ar}}{\partial \xi^2}\right) = m_n \frac{\partial^2 w_{ar}}{\partial t_n^2} \end{aligned}\right\} \tag{A.7}$$

where $2u_{sr} = u_{nh} + u_{n1}/R_{ht}$, and $2N_{sr} = N_{nh} + N_{n1}/R_{ht}$. Other definitions are the same as those of the shear lag rod model with identical adherends, and the host beam extension is solved: $u_{nh} = 2(u_{sr} + u_{ar})/(1 + R_{ht})$.

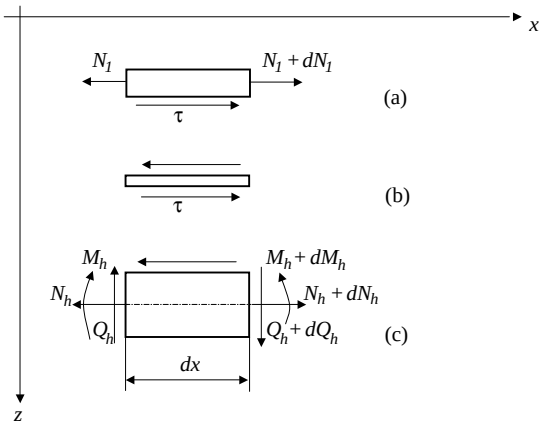

Fig. 3. A shear lag rod model for a host beam with one PZT patch. (a) PZT infinitesimal element, (b) adhesive layer and (c) host beam infinitesimal element.

The characteristic equation can also be expressed by Eq. (19) except:

$$\alpha_a = \sqrt{\frac{r_{\tau a}(1+R_{ht})}{m_T}} \quad \text{and} \quad \beta_{aw} = \frac{r_h \alpha_a}{2\alpha_w \sqrt{1+R_{ht}}} \tag{A.8}$$

Using the same solution procedure, solutions of U_{sr}, U_{ar} and W_{ar} can be obtained as given in Eqs. (34) and (38) with β_1, β_2, and β_3 being replaced by the new solved eigenvalues.

A.2. A host beam with two symmetrically bonded PZT patches

When the two PZT patches are symmetrically bonded to the host beam as shown in Fig. 4, we can develop the following formulations for the shear lag rod model.

The non-dimensional dynamic equilibrium equations are:

$$\left.\begin{aligned} &r_h \frac{\partial N_{n1}}{\partial \xi} + \tau_{n1} = \frac{r_1}{r_h} m_n \frac{\partial^2 u_{n1}}{\partial t_n^2}, \quad r_h \frac{\partial N_{n2}}{\partial \xi} - \tau_{n2} = \frac{r_1}{r_h} m_n \frac{\partial^2 u_{n2}}{\partial t_n^2} \\ &r_h \frac{\partial N_{nh}}{\partial \xi} - \tau_{n1} + \tau_{n2} = m_n \frac{\partial^2 u_{nh}}{\partial t_n^2}, \quad r_h \frac{\partial Q_{nh}}{\partial \xi} = m_n \frac{\partial^2 w_{nh}}{\partial t_n^2}, \quad \frac{\partial M_{nh}}{\partial \xi} + \frac{\tau_{n1} + \tau_{n2}}{2} - Q_{nh} = 0 \end{aligned}\right\} \tag{A.9}$$

The constitutive relations of the adhesives are given by:

$$\tau_{n1} = r_{\tau a}\left[(u_{nh} - u_{n1}) + \frac{r_h}{2}\frac{\partial w_{nh}}{\partial \xi}\right], \quad \tau_{n2} = r_{\tau a}\left[(u_{n2} - u_{nh}) + \frac{r_h}{2}\frac{\partial w_{nh}}{\partial \xi}\right] \tag{A.10}$$

The dynamic equilibrium equations and the constitutive relations can be transferred into two sets of the independent equations that can be separately solved.

Case 1: Extensional motion of the host beam

When the host beam undergoes extensional motion only, we have the following set of equations by introducing the transforming parameters:

$$2N_{ps} = N_{n1} + N_{n2}, \quad 2u_{ps} = u_{n1} + u_{n2}, \quad 2\tau_{ps} = \tau_{n1} - \tau_{n2}, \quad 2V_{ps} = V_1 + V_2 \tag{A.11}$$

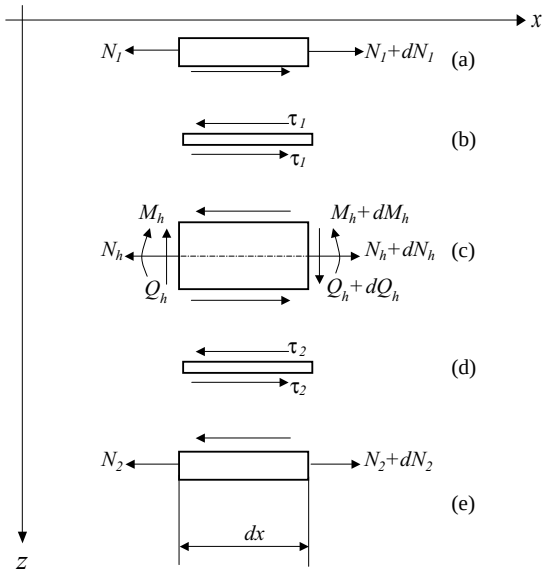

Fig. 4. A shear lag rod model for a host beam with two symmetrically bonded PZT patches. (a) PZT1 infinitesimal element, (b) adhesive layer 1, (c) host beam infinitesimal element, (d) adhesive layer 2 and (e) PZT2 infinitesimal element.

The dynamic equilibrium equations are:

$$r_h \frac{\partial N_{ps}}{\partial \xi} + \tau_{ps} = \frac{r_1}{r_h} m_n \frac{\partial^2 u_{ps}}{\partial t_n^2}, \quad r_h \frac{\partial N_{nh}}{\partial \xi} - 2\tau_{ps} = m_n \frac{\partial^2 u_{nh}}{\partial t_n^2} \tag{A.12}$$

The constitutive relations are given by:

$$N_{ps} = E_{nh} r_1 \frac{\partial u_{ps}}{\partial \xi} + \frac{e_{31} V_{ps}}{G_a L}, \quad N_{nh} = E_{nh} r_h \frac{\partial u_{nh}}{\partial \xi}, \quad \tau_{ps} = r_{\tau a}(u_{nh} - u_{ps}) \tag{A.13}$$

The decoupled dynamic equations (A.15) and (A.16) are finally obtained by substituting Eq. (A.13) into (A.12) and introducing the following relations:

$$2u_{ss} = u_{nh} + 2u_{ps}/R_{ht}, \quad 2u_{sa} = u_{nh} - u_{ps}, \quad \tau_{ps} = 2r_{\tau a} u_{sa} \tag{A.14}$$

$$E_{nh} r_h^2 \frac{\partial^2 u_{ss}}{\partial \xi^2} = m_n \frac{\partial^2 u_{ss}}{\partial t_n^2} \tag{A.15}$$

$$E_{nh} r_h^2 \frac{\partial^2 u_{sa}}{\partial \xi^2} - (2 + R_{ht}) r_{\tau a} u_{sa} = m_n \frac{\partial^2 u_{sa}}{\partial t_n^2} \tag{A.16}$$

Eqs. (A.15) and (A.16) can be separately solved, and then the extensional motions are obtained by referring to the relations shown in Eqs. (A.11) and (A.14). Incorporating with dynamic solutions of the host beam where no PZT patches are bonded and considering the continuity condition, we can obtain the extensional motion of the host beam. The other quantities of the smart beam can also be readily obtained following the same procedure as that of solutions to the present PSM model.

When both PZTs are used as actuators, the extensional motion can be achieved by applying a voltage $V_s(t_n)$ of the same magnitude to both PZT patches so that the electric fields in both PZTs are in the same direction at any time.

Case 2: Flexural motion of the host beam

When the host beam undergoes the flexural motion only, the following transforming parameters are used:

$$2N_{pa} = N_{n1} - N_{n2}, \quad 2u_{pa} = u_{n1} - u_{n2}, \quad 2\tau_{pa} = \tau_{n1} + \tau_{n2}, \quad 2V_{pa} = V_1 - V_2 \tag{A.17}$$

The dynamic equations are:

$$\left.\begin{aligned} &r_h \frac{\partial N_{pa}}{\partial \xi} + \tau_{pa} = \frac{r_1}{r_h} m_n \frac{\partial^2 u_{pa}}{\partial t_n^2} \\ &r_h \frac{\partial Q_{nh}}{\partial \xi} = m_n \frac{\partial^2 w_{nh}}{\partial t_n^2}, \quad \frac{\partial M_{nh}}{\partial \xi} + \tau_{pa} - Q_{ph} = 0 \end{aligned}\right\} \tag{A.18}$$

and the constitutive relations are given by:

$$N_{pa} = E_{nh} r_h \frac{\partial u_{pa}}{\partial \xi} + \frac{e_{31} V_{pa}}{G_a h}, \quad M_{nh} = -\frac{1}{12} E_{nh} r_h^3 \frac{\partial^2 w_{nh}}{\partial \xi^2}, \quad \tau_{pa} = r_{\tau a}\left(- u_{pa} + \frac{r_h}{2} \frac{\partial w_{nh}}{\partial \xi} \right) \tag{A.19}$$

The motions equations are then transferred into:

$$\left.\begin{aligned} &E_{nh} r_h^2 \frac{\partial^2 u_{pa}}{\partial \xi^2} + R_{ht} r_{\tau a}\left(- u_{pa} + \frac{r_h}{2} \frac{\partial w_{nh}}{\partial \xi} \right) = m_n \frac{\partial^2 u_{pa}}{\partial t_n^2} \\ &-\frac{E_{nh} r_h^4}{12} \frac{\partial^4 w_{nh}}{\partial \xi^4} + R_{ht} r_{\tau a} \frac{r_h}{R_{ht}}\left(- \frac{\partial u_{pa}}{\partial \xi} + \frac{r_h}{2} \frac{\partial^2 w_{nh}}{\partial \xi^2} \right) = m_n \frac{\partial^2 w_{nh}}{\partial t_n^2} \end{aligned}\right\} \tag{A.20}$$

The characteristic equation is expressible by Eq. (19) except for:

$$\alpha_a = \sqrt{\frac{r_{\tau a} R_{ht}}{m_T}} \quad \text{and} \quad \beta_{aw} = \frac{r_h \alpha_a}{\alpha_w \sqrt{2 R_{ht}}} \tag{A.21}$$

When both PZTs are used as actuators, the flexural motion can be achieved by applying a voltage $V_s(t_n)$ of the same magnitude but opposite phase to PZT1 and PZT2 so that the electric fields in both PZTs are opposite in direction at any time.

In this case, different equations from those of the exact dynamic solutions including peel stresses are given as follows.

Eq. (37) becomes:

$$\left.\begin{aligned} K_1 &= \beta_1 K_{10} = -\frac{r_h}{2} \frac{\beta_1 \beta_{au}^2}{\beta_1^2 - (\beta_{au}^2 - \beta_{\omega u}^2)} \\ K_2 &= \beta_2 K_{20} = -\frac{r_h}{2} \frac{\beta_2 \beta_{au}^2}{\beta_2^2 - (\beta_{au}^2 - \beta_{\omega u}^2)} \\ K_3 &= \beta_3 K_{30} = -\frac{r_h}{2} \frac{\beta_3 \beta_{au}^2}{\beta_3^2 + (\beta_{au}^2 - \beta_{\omega u}^2)} \end{aligned}\right\} \tag{A.22}$$

Eqs. (41) and (42) are rewritten as:

$$\left.\begin{aligned} K_{\beta 1} &= \beta_1 \left[\beta_1^2 + \frac{12 r_{\tau a}}{E_{nh} r_h^3} \left(K_{10} - \frac{r_h}{2} \right) \right] \\ K_{\beta 2} &= \beta_2 \left[\beta_2^2 + \frac{12 r_{\tau a}}{E_{nh} r_h^3} \left(K_{20} - \frac{r_h}{2} \right) \right] \\ K_{\beta 3} &= \beta_3 \left[\beta_3^2 + \frac{12 r_{\tau a}}{E_{nh} r_h^3} \left(K_{30} + \frac{r_h}{2} \right) \right] \end{aligned}\right\} \tag{A.23}$$

$$\left.\begin{aligned} B_{a2} &= \frac{1}{\Delta_a}[\Delta_{N2}(\varepsilon_p) + \Delta_{M2}(-\varepsilon_M) + \Delta_{Q2}(-\varepsilon_Q)] \\ B_{a4} &= \frac{1}{\Delta_a}[\Delta_{N4}(\varepsilon_p) + \Delta_{M4}(-\varepsilon_M) + \Delta_{Q4}(-\varepsilon_Q)] \\ B_{a5} &= \frac{1}{\Delta_a}[\Delta_{N5}(\varepsilon_p) + \Delta_{M5}(-\varepsilon_M) + \Delta_{Q5}(-\varepsilon_Q)] \end{aligned}\right\} \tag{A.24}$$

Eqs. (43) and (44) are degenerated as:

$$W_{nh}(1) = W_{nh\mathrm{II}}(0), \quad \frac{\mathrm{d}W_{nh}(1)}{\mathrm{d}\xi} = \frac{\mathrm{d}W_{nh\mathrm{II}}(0)}{\mathrm{d}\xi} \tag{A.25}$$

Eq. (45) is simplified as

$$\left.\begin{aligned} b_{22}\varepsilon_M + b_{23}\varepsilon_Q &= c_{2e}\varepsilon_p + c_{2P}\varepsilon_P \\ b_{32}\varepsilon_M + b_{33}\varepsilon_Q &= c_{3e}\varepsilon_p + c_{3P}\varepsilon_P \end{aligned}\right\} \tag{A.26}$$

and the related coefficients can be simplified accordingly.

The partial differential form of motion equations can be obtained for the peel stress model with different cross sections and two symmetric PZT patches. Following the same procedure to that of the identical composite smart beam and performing the similar transformation to that in the static analysis for two symmetric PZT patches, the equations are simplified into two sets of independent equations, of which one is an 8-order differential equation. By assuming the harmonic motion, a four order polynomial equation can be obtained and analytically solved. However, analysis of the solution forms and the determinations of the integration constants are too complicated to conduct practically.

Appendix B. The intersectional displacements of the host beam and the coefficients of Eq. (45)

The expressions for the intersectional displacements of the host beam are:

$$\left.\begin{aligned} U_{nh\mathrm{II}}(0) &= \frac{\varepsilon_N \cos\beta_{s1}\alpha_p - \varepsilon_F}{\beta_{s1}\sin\beta_{s1}\alpha_p} \\ W_{nh\mathrm{II}}(0) &= \frac{1}{\beta_h^3(\cosh\beta_h\alpha_p\cos\beta_h\alpha_p - 1)}[-\beta_h\varepsilon_M\sinh\beta_h\alpha_p\sin\beta_h\alpha_p + \\ &\quad \varepsilon_Q(\sinh\beta_h\alpha_p\cos\beta_h\alpha_p - \cosh\beta_h\alpha_p\sin\beta_h\alpha_p) - \varepsilon_P(\sinh\beta_h\alpha_p - \sin\beta_h\alpha_p)] \\ \frac{\mathrm{d}W_{nh\mathrm{II}}(0)}{\mathrm{d}\xi} &= \frac{1}{\beta_h^2(\cosh\beta_h\alpha_p\cos\beta_h\alpha_p - 1)}[\beta_h\varepsilon_M(\sinh\beta_h\alpha_p\cos\beta_h\alpha_p + \cosh\beta_h\alpha_p\sin\beta_h\alpha_p) \\ &\quad + \varepsilon_Q\sinh\beta_h\alpha_p\sin\beta_h\alpha_p + \varepsilon_P(\cosh\beta_h\alpha_p - \cos\beta_h\alpha_p)] \end{aligned}\right\} \tag{B.1}$$

$$\left.\begin{aligned} U_s(1) &= \frac{(\varepsilon_N + \varepsilon_p)\tan\beta_{s1}}{2\beta_{s1}} \\ W_s(1) &= \frac{-\beta_e\varepsilon_M(\cosh 2\beta_e - \cos 2\beta_e) + \varepsilon_Q(\sinh 2\beta_e - \sin 2\beta_e)}{4\beta_e^3(\cosh 2\beta_e + \cos 2\beta_e)} \\ \frac{\mathrm{d}W_s(1)}{\mathrm{d}\xi} &= \frac{-2\beta_e\varepsilon_M(\sinh 2\beta_e + \sin 2\beta_e) + \varepsilon_Q(\cosh 2\beta_e - \cos 2\beta_e)}{4\beta_e^2(\cosh 2\beta_e + \cos 2\beta_e)} \end{aligned}\right\} \tag{B.2}$$

$$\left.\begin{aligned}
U_a(1) &= \frac{1}{2\Delta_a}\{[\Delta_{N2}f_{u2}(1)+\Delta_{N4}f_{u4}(1)+\Delta_{N5}f_{u5}(1)](\varepsilon_N-\varepsilon_p)-[\Delta_{M2}f_{u2}(1)+\Delta_{M4}f_{u4}(1)\\
&\quad +\Delta_{M5}f_{u5}(1)]\varepsilon_M-[\Delta_{Q2}f_{u2}(1)+\Delta_{Q4}f_{u4}(1)+\Delta_{Q5}f_{u5}(1)]\varepsilon_Q\}\\
W_a(1) &= \frac{1}{2\Delta_a}\{[\Delta_{N2}f_{w2}(1)+\Delta_{N4}f_{w4}(1)+\Delta_{N5}f_{w5}(1)](\varepsilon_N-\varepsilon_p)-[\Delta_{M2}f_{w2}(1)+\Delta_{M4}f_{w4}(1)\\
&\quad +\Delta_{M5}f_{w5}(1)]\varepsilon_M-[\Delta_{Q2}f_{w2}(1)+\Delta_{Q4}f_{w4}(1)+\Delta_{Q5}f_{w5}(1)]\varepsilon_Q\}\\
\frac{\mathrm{d}W_a(1)}{\mathrm{d}\xi} &= \frac{1}{2\Delta_a}\{[\Delta_{N2}f_{d2}(1)+\Delta_{N4}f_{d4}(1)+\Delta_{N5}f_{d5}(1)](\varepsilon_N-\varepsilon_p)-[\Delta_{M2}f_{d2}(1)+\Delta_{M4}f_{d4}(1)\\
&\quad +\Delta_{M5}f_{d5}(1)]\varepsilon_M-[\Delta_{Q2}f_{d2}(1)+\Delta_{Q4}f_{d4}(1)+\Delta_{Q5}f_{d5}(1)]\varepsilon_Q\}
\end{aligned}\right\} \tag{B.3}$$

where

$$\left.\begin{aligned}
f_{u2}(1) &= K_1\sinh\beta_1-K_3\sin\beta_3\\
f_{u4}(1) &= K_2\sinh\beta_2-K_3\sin\beta_3\\
f_{u5}(1) &= K_1K_{31}\cosh\beta_1+K_2K_{32}\cosh\beta_2-K_3\cos\beta_3
\end{aligned}\right\} \tag{B.4}$$

$$\left.\begin{aligned}
f_{w2}(1) &= \cosh\beta_1-\cos\beta_3\\
f_{w4}(1) &= \cosh\beta_2-\cos\beta_3\\
f_{w5}(1) &= K_{31}\sinh\beta_1+K_{32}\sinh\beta_2+\sin\beta_3
\end{aligned}\right\} \tag{B.5}$$

$$\left.\begin{aligned}
f_{d2}(1) &= \beta_1\sinh\beta_1+\beta_3\sin\beta_3\\
f_{d4}(1) &= \beta_2\sinh\beta_2+\beta_3\sin\beta_3\\
f_{d5}(1) &= \beta_1K_{31}\cosh\beta_1+\beta_2K_{32}\cosh\beta_2+\beta_3\cos\beta_3
\end{aligned}\right\} \tag{B.6}$$

The coefficients of Eq. (45) are given by:

$$\left.\begin{aligned}
b_{11} &= -\frac{c\tan\beta_{s1}\alpha_p}{\beta_{s1}}+\frac{\tan\beta_{s1}}{2\beta_{s1}}+\frac{1}{2\Delta_a}[\Delta_{N2}f_{u2}(1)+\Delta_{N4}f_{u4}(1)+\Delta_{N5}f_{u5}(1)]\\
b_{12} &= -\frac{1}{2\Delta_a}[\Delta_{M2}f_{u2}(1)+\Delta_{M4}f_{u4}(1)+\Delta_{M5}f_{u5}(1)]\\
b_{13} &= -\frac{1}{2\Delta_a}[\Delta_{Q2}f_{u2}(1)+\Delta_{Q4}f_{u4}(1)+\Delta_{Q5}f_{u5}(1)]
\end{aligned}\right\} \tag{B.7}$$

$$\left.\begin{aligned}
b_{21} &= \frac{1}{2\Delta_a}[\Delta_{N2}f_{w2}(1)+\Delta_{N4}f_{w4}(1)+\Delta_{N5}f_{w5}(1)]\\
b_{22} &= \frac{\sinh\beta_h\alpha_p\sin\beta_h\alpha_p}{\beta_h^2(\cosh\beta_h\alpha_p\cos\beta_h\alpha_p-1)}-\frac{(\cosh2\beta_e-\cos2\beta_e)}{4\beta_e^2(\cosh2\beta_e+\cos2\beta_e)}\\
&\quad -\frac{1}{2\Delta_a}[\Delta_{M2}f_{w2}(1)+\Delta_{M4}f_{w4}(1)+\Delta_{M5}f_{w5}(1)]\\
b_{23} &= -\frac{\sinh\beta_h\alpha_p\cos\beta_h\alpha_p-\cosh\beta_h\alpha_p\sin\beta_h\alpha_p}{\beta_h^3(\cosh\beta_h\alpha_p\cos\beta_h\alpha_p-1)}+\frac{(\sinh2\beta_e-\sin2\beta_e)}{4\beta_e^3(\cosh2\beta_e+\cos2\beta_e)}\\
&\quad -\frac{1}{2\Delta_a}[\Delta_{Q2}f_{w2}(1)+\Delta_{Q4}f_{w4}(1)+\Delta_{Q5}f_{w5}(1)]
\end{aligned}\right\} \tag{B.8}$$

$$\left.\begin{aligned}
b_{31} &= \frac{1}{2\Delta_a}[\Delta_{N2}f_{d2}(1) + \Delta_{N4}f_{d4}(1) + \Delta_{N5}f_{d5}(1)] \\
b_{32} &= -\frac{\sinh\beta_h\alpha_p\cos\beta_h\alpha_p + \cosh\beta_h\alpha_p\sin\beta_h\alpha_p}{\beta_h(\cosh\beta_h\alpha_p\cos\beta_h\alpha_p - 1)} - \frac{(\sinh 2\beta_e + \sin 2\beta_e)}{2\beta_e(\cosh 2\beta_e + \cos 2\beta_e)} \\
&\quad - \frac{1}{2\Delta_a}[\Delta_{M2}f_{d2}(1) + \Delta_{d4}f_{w4}(1) + \Delta_{M5}f_{d5}(1)] \\
b_{33} &= -\frac{\sinh\beta_h\alpha_p\sin\beta_h\alpha_p}{\beta_h^2(\cosh\beta_h\alpha_p\cos\beta_h\alpha_p - 1)} + \frac{(\cosh 2\beta_e - \cos 2\beta_e)}{4\beta_e^2(\cosh 2\beta_e + \cos 2\beta_e)} \\
&\quad - \frac{1}{2\Delta_a}[\Delta_{Q2}f_{d2}(1) + \Delta_{Q4}f_{w4}(1) + \Delta_{Q5}f_{d5}(1)]
\end{aligned}\right\} \tag{B.9}$$

$$\left.\begin{aligned}
c_{1e} &= -\frac{\tan\beta_{s1}}{2\beta_{s1}} + \frac{1}{2\Delta_a}[\Delta_{N2}f_{u2}(1) + \Delta_{N4}f_{u4}(1) + \Delta_{N5}f_{u5}(1)] \\
c_{1F} &= -\frac{1}{\beta_{s1}\sin\beta_{s1}\alpha_p}
\end{aligned}\right\} \tag{B.10}$$

$$\left.\begin{aligned}
c_{2e} &= \frac{1}{2\Delta_a}[\Delta_{N2}f_{w2}(1) + \Delta_{N4}f_{w4}(1) + \Delta_{N5}f_{w5}(1)] \\
c_{2P} &= -\frac{\sinh\beta_h\alpha_p - \sin\beta_h\alpha_p}{\beta_h^3(\cosh\beta_h\alpha_p\cos\beta_h\alpha_p - 1)}
\end{aligned}\right\} \tag{B.11}$$

$$\left.\begin{aligned}
c_{3e} &= \frac{1}{2\Delta_a}[\Delta_{N2}f_{d2}(1) + \Delta_{N4}f_{d4}(1) + \Delta_{N5}f_{d5}(1)] \\
c_{3P} &= \frac{\cosh\beta_h\alpha_p - \cos\beta_h\alpha_p}{\beta_h^2(\cosh\beta_h\alpha_p\cos\beta_h\alpha_p - 1)}
\end{aligned}\right\} \tag{B.12}$$

References

Crawley, E.F., Anderson, E.H., 1990. Detailed models of piezoceramic actuation of beams. Journal of Intelligent Material Systems and Structures 1, 4–25.

Crawley, E.F., de Luis, J., 1987. Use of piezoelectric actuators as elements of intelligent structures. AIAA Journal 25 (10), 1373–1385.

Gibbs, G.P., Fuller, C.R., 1992. Excitation of thin beams using asymmetric piezoelectric actuators. Journal of the Acoustic Society of America 92 (6), 3221–3227.

Goland, M., Reissner, E., 1944. The stresses in cemented joints. Journal of Applied Mechanics 11, A-17–A-27.

Im, S., Atluri, S.N., 1989. Effects of a piezo-actuator on a finitely deformed beam subjected to general loading. AIAA Journal 27 (12), 549–564.

Irschik, H., Krommer, K., Pichler, U., 1999. Shaping of distributed piezoelectric sensors for flextural vibrations of smart beams. In: Varadan, V.V. (Ed.), Proceedings of SPIE'S Sixth Annual International Symposium on Smart Structures and Materials, vol. 3667. SPIE, Newport Beach, CA, pp. 418–426.

Kugel, V.D., Xu, B., Zhang, Q.M., Cross, L.E., 1998. Bimorph-based piezoelectric air acoustic transducer: model. Sensors and Actuators A: Physics 69, 234–242.

Lim, C.W., He, L.H., Soh, A.K., 2001. Three-dimensional electric responses of a parallel piezoelectric bimorph. International Journal of Solids and Structures 38, 2833–2849.

Luo, Q., Tong, L., 2002a. Exact static solutions to piezoelectric smart beams including peel stresses. Part I: Theoretical formulation. International Journal of Solids and Structures 39 (18), 4677–4695.

Luo, Q., Tong, L., 2002b. Exact static solutions to piezoelectric smart beams including peel stresses. Part II: Numerical results, comparison and discussion. International Journal of Solids and Structures 39 (18), 4697–4722.

Morris, C.J., Forster, F.K., 2000. Optimization of a circular piezoelectric bimorph for a micropump driver. Journal of Micromechanics and Microengineering 10, 459–465.

Rizet, N., Brissaud, M., Gonnard, P., Bera, J.C., Sunyach, M., 2000. Modal control of beam flexural vibration. Journal of the Acoustic Society of America 107 (4), 2061–2067.

Shi, G., Atluri, S.N., 1990. Active control of nonlinear dynamic response of space-frames using piezo-electric actuators. Computers and Structures 34 (4), 1801–1807.

Smits, J.G., Dalke, S.I., Cooney, T.K., 1991. The constituent equations of piezoelectric bimorphs. Sensors and Actuators A: Physics 28, 41–61.

Tiersten, H.F., 1969. Linear Piezoelectric Plate Vibrations—Element of Linear Theory of Piezoelectricity and the Vibrations of Piezoelectric Plates. Plenum Press, New York.

Thomson, W.T., 1998. Theory of Vibration with Applications, fourth ed Stanley Thornes, Cheltenham, UK.

Timoshenko, S.P., Gere, J.M., 1972. Mechanics of Materials. Van Nostrand Reinhold Co., New York.

Wang, Q.M., Cross, L.E., 1999. Constitutive equations of symmetrical triple layer piezoelectric benders. IEEE Transaction on Ultrasonics, Ferroelectrics, and Frequency Control 46 (6), 1343–1351.